Progress In Electromagnetics Research C, Vol. 89, 75–85, 2019

Pixel Shape Ground Inspired Frequency Reconfigurable Antenna

Ajay Yadav[1, 2, *], Minakshi Tewari[1], and Rajendra P. Yadav[2]

Abstract—A microstrip antenna with a pixel ground structure for single and multiband frequency reconfigurable applications is presented. The partial ground structure of the primary antenna is converted into pixel shapes which produce single and multiband frequency reconfigurable characteristics by the means of RF switches. The designed antenna operations are switchable over multiband, single frequency band and UWB spectrum with the distinct configuration of RF switches. Three cases of RF switch configurations have been demonstrated with their simulated and measured results to verify the reconfigurable characteristics.

1. INTRODUCTION

Multiband antennas are greatly appreciated in current wireless communication scenario due to their huge demand in mobile communications and remote sensing applications. A significant drawback of conventional multiband antennas is that they function for specific operations at a time, and for different applications each time a new antenna with desired frequency applications is required, so they increase the system cost. Nowadays, reconfigurable antennas are highly demanded to overcome the described problems. The reconfigurable antennas can function for multiple operations with a single antenna. Reconfigurable antennas are defined with the capability of modifying one or more antenna parameters without affecting other antenna properties [1–4]. UWB antennas suffer from electromagnetic interferences due to narrowband applications in 3.1–10.6 GHz frequency range. Reconfigurable antennas are designed to play a key role in controlling the responses of antennas and limit the disadvantage of UWB antennas. Recently, pixel patches are highly appreciated in the design of reconfigurable antennas. Pixel shaped parasitic elements have been used to steer the antenna beam without using phase shifter in [1]. For pattern reconfigurable applications of a steerable beam in desired directions and for multi-function operations, a reconfigurable parasitic pixel surface has been utilized [2, 3]. Pixel shaped parasitic elements are used to design antennas with diverse or multi-function characteristics like frequency, polarization and pattern as discussed in [4–7]. Nonuniform pixels are a matter of concern to develop a variety of configurations, and one of them has been presented in [8], which produces frequency diversity. As we have discussed so far, pixel structure parasitic elements are very interesting in design diversity of antenna parameters, so they require to be optimized through specific algorithms as discussed in [9–11] and [11]. Pixel parasitic element concept is also useful for producing hybrid type of reconfigurability or the most popular pattern diversity as discussed in [12–14]. The use of a reconfigurable pixel-layer isolator to dynamically regulate the mutual coupling between the two antennas in the repeater to achieve frequency diversity is presented in [15]. A DGS based frequency reconfigurable antenna is discussed in [18].

The pixel shape structures of an antenna (on a radiating patch or on the ground or as parasitic one) exhibit the highest reconfiguration capability, but its implementation is limited due to a huge number of RF switches [16].

Received 21 August 2018, Accepted 6 December 2018, Scheduled 21 December 2018

* Corresponding author: Ajay Yadav (ajayrfmicrowave@gmail.com).
[1] Department of ECE, Global Institute of Technology, Jaipur, India. [2] Department of ECE, Malaviya National Institute of Technology Jaipur, India.

The paper presents a single and multiband frequency switchable antenna with a single configuration of switches. However, to the best of the authors' knowledge, previously very few frequency reconfigurable antennas were available with multiband resonance functions as well as wide-band applications (UWB). The presented antenna is capable to function for multiband frequencies, single resonance frequency and UWB spectrum with distinct RF switch configurations, which are rarely found with previously proposed antennas. In this paper, we demonstrate 11 cases of prospective RF switch combinations, and among them, 4 cases have been fabricated and measured to verify the concept. However, it is possible to design N^2 combinations of RF switches and develop antenna applications accordingly. Here we use a metal strip to show the PIN diode in ON condition and remove a metal strip for OFF condition. Likewise, the reflection coefficient of proposed antenna has been compared to a special configuration of antenna using metal strip and PIN diode.

2. ANTENNA DESIGN SIMULATION AND ANALYSIS

2.1. Antenna Design

The proposed reconfigurable antenna is displayed in Fig. 1. Fig. 1(a) depicts a front view, and Fig. 1(b) presents the bottom side view of the antenna. The primary antenna radiates over the UWB spectrum as discussed in [17], and it is reproduced to design the pixel shape reconfigurable antenna. The antenna is printed on an FR-4 dielectric material with thickness 1.6 mm, permittivity $\varepsilon_r = 4.4$ and loss tangent 0.02. In the simulation, PIN diodes are used to demonstrate the frequency reconfigurability. The proposed antenna is simulated and optimized using commercially available Ansoft's HFSS simulator.

The suggested antenna has a compact size of $42.5 \times 34\,\text{mm}^2$. A rectangular patch with steps near

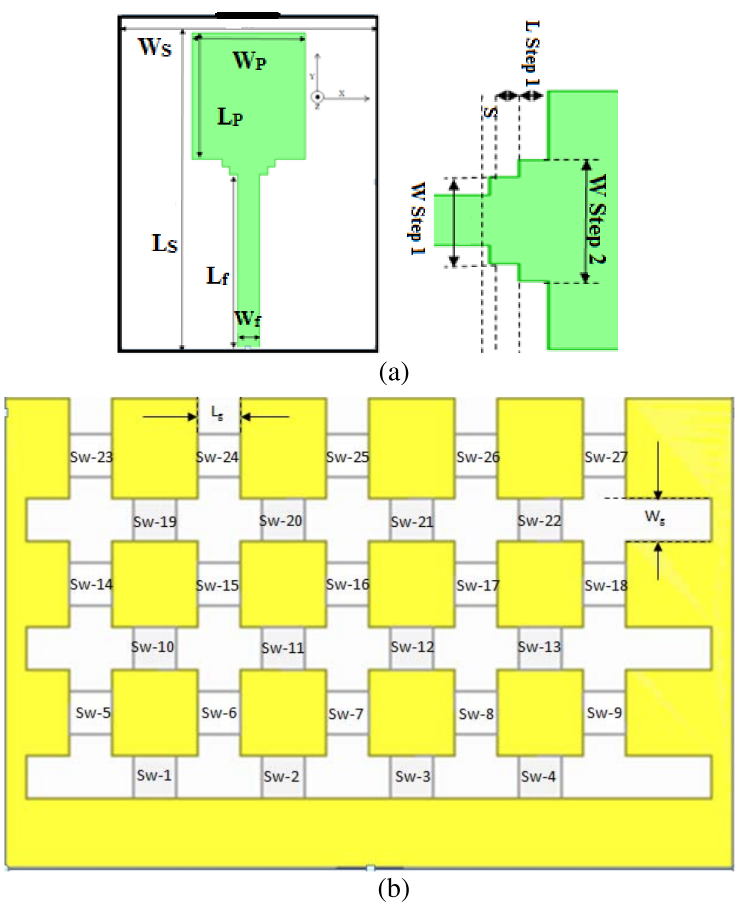

Figure 1. Design and configuration of proposed antenna. (a) Front view. (b) Back view.

feedline and partial ground is chosen as a primary antenna which resonates for complete UWB (3.1–10.6 GHz) spectrum [17]. To make this antenna single and multiband resonance, the partial ground of primary antenna is converted into reconfigurable pixel shapes which produce a resonance for multiband and for high-frequency band (X-band). All related dimensions are offered in Table 1.

Table 1. Optimized dimensions of proposed antenna.

Variable	W_S	L_S	W_P	L_P	W_f	L_g
Size (mm)	34	42.5	15	16	3	2
W_G	L_f	S	L_{Step1}	W_{Step1}	W_{Step2}	W_g
34	22	0.2	1	5	7	2

2.2. Investigation of Antenna

Figure 2 represents different RF switch configurations to produce multiband, single resonance and UWB spectrum antennas. However, these configurations can be made reconfigurable with the help of RF switches (PIN diodes). Here we simulate the mentioned configurations with PIN diode specifications.

Various potential cases of proposed antenna with RF PIN diodes configurations are demonstrated in Fig. 2, and their details are listed in Table 2. In Fig. 2, diodes with OFF condition are presented by **Green color** whereas diodes with ON condition are with **dark Blue color**. However, to maintain UWB characteristics, initially all diodes are kept in ON condition, and to achieve single band resonance or multiband resonance, diodes are featured with various combinations of diodes in OFF conditions [16]. All PIN diodes (BAR 50-02 V) are kept with 3 Ω resistance for ON condition and 5 KΩ resistance and 0.15 pF capacitor for OFF condition.

Table 2. Diode switching configurations.

Antenna	**Diodes in OFF Condition**
Case-1	D-2, D-3, D-6, D-7 and D-8
Case-2	D-2, D-3, D-6, D-7, D-8, D-11 and D-12
Case-3	D-2, D-3, D-6, D-7, D-8, D-11, D-12, D-15, D-16 and D-17
Case-4	D-2, D-3, D-6, D-7, D-8, D-11, D-12, D-15, D-16, D-17, D-20 and D-21
Case-5	D-2, D-3, D-6, D-7, D-8, D-11, D-12, D-15, D-16, D-17, D-20, D-21 and D-25
Case-6	D-5, D-6, D-7, D-8, D-9D-14, D-18, D-23 and D-27
Case-7	D-23, D-24, D-25, D-26, D-27, D-2, D-3, D-11, D-12, D-20 and D-21
Case-11	D-1, D-2, D-3, D-4, D-5, D-6, D-7, D-8, D-9, D-11, D-12, D-20 and D-21
Case-8	ALL SWITCH ARE OFF
Case-9	D-5, D-6, D-7, D-8, D-9, D-14, D-15, D-16, D-17, D-18, D-23, D-25 and D-27 ON
Case-10	D-5, D-9, D-14, D-18, D-23 and D-27 ON

When Case-1 and Case-10 are implemented, slot created between pixels makes a positive condition [16] (changes the effective capacitance of the primary antenna) to resonate antenna at 5.2–5.6 GHz (WLAN Band) whereas Case-9 produces multiband functions. When Case-2 and Case-7 are implemented, the antenna resonates for multiband frequencies at C- Band Uplink frequency band and X-band frequencies for satellite communications. When Case-3, Case-4, and Case-11 are implemented, the antenna resonates for 7 GHz to 7.8 GHz (X-band downlink frequency band for satellite Communications). When Case-5 is used, the antenna radiates at 9.4 GHz. Case-6 is useful for broadband applications, which is used to radiate antenna at 2.8 GHz to 8 GHz frequency, and Case-8 antenna radiates at 5.5 to 9 GHz frequency band.

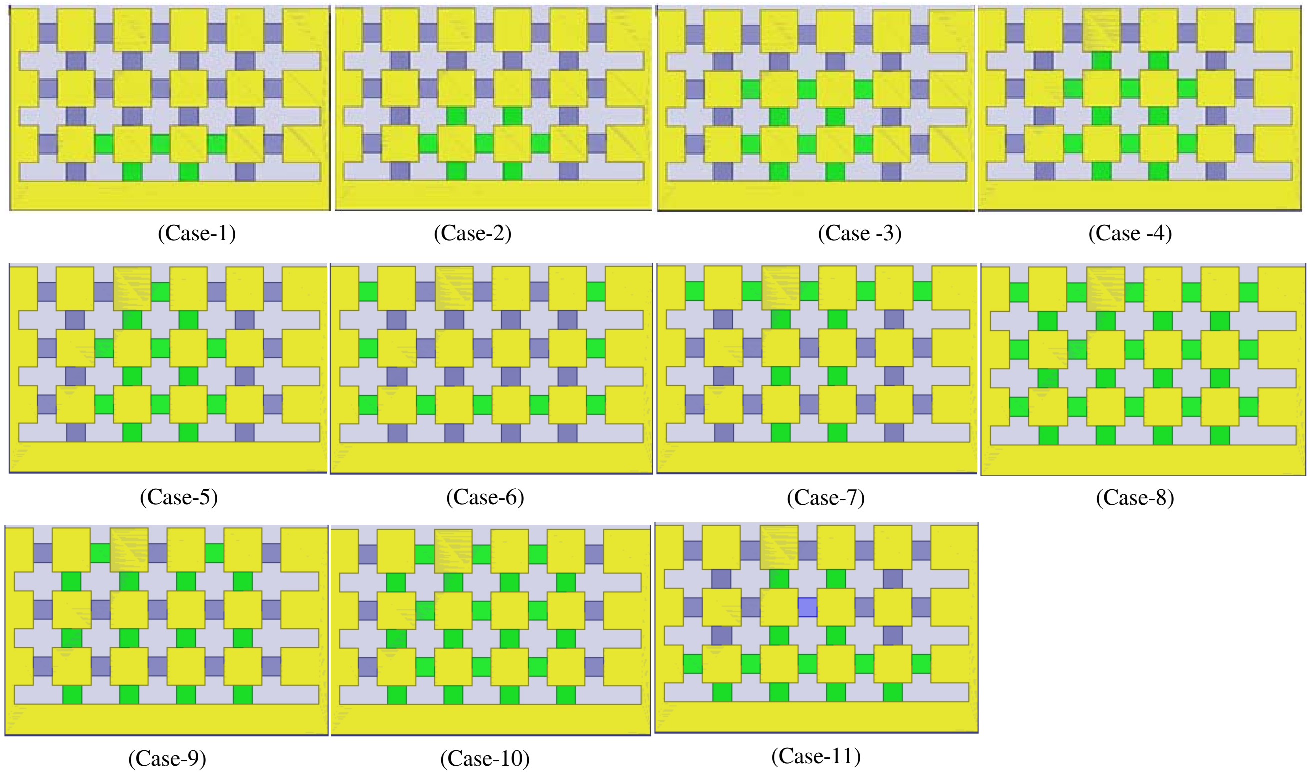

Figure 2. Frequency reconfigurable antennas with various PIN diode configurations [16].

3. DISCUSSION OF SIMULATED RESULTS

The simulated S_{11} (in dB) results of the proposed antenna with the distinct diode combinations are presented. The cases discussed in Table 2 for distinct diode combinations are presented in Figs. 3(a)–(d). In Fig. 3(a), Case-1, Case-2, and Case-3 S_{11} (in dB) results with respective diode combinations are presented. From Fig. 3(a), the diodes combination in Case-1 can be used to operate antenna for single frequency band (WLAN) whereas Case-2 and Case-3 can be used to operate antenna for multiband (triple) resonant frequencies (5.8/7.8/9.6 GHz). Fig. 3(b) shows that the proposed antenna can be used for multiband operations (triple band as well as dual-band) with diode configurations discussed for Case-5 and Case-4, respectively. Similarly, from Fig. 3(c), the proposed antenna can be used for dual or triple band applications with diode configurations mentioned for Case-6, Case-7, and Case-8 for pixel ground. From Fig. 3(c) the proposed antenna can be used for WiMAX, X-band downlink frequency and higher frequency (9.6 GHz) applications using Case-8 diode combinations. Fig. 3(d) shows the diode combinations for Case-9, Case-10, and Case-11 which can be used for broadband applications. Case-9 can be used to operate an antenna for multiband applications while Case-10 and Case-11 can be for broadband applications including UWB spectrum.

The primary antenna is a partial ground microstrip patch antenna which operates over the UWB spectrum with VSWR < 2 [17]. We have simulated, fabricated and measured the primary antenna which shows desired results. The fabricated prototype of primary antenna is presented in Fig. 4. We use the partial ground structure of the primary antenna to convert it into pixel shapes to produce multiband, single band and UWB spectrum applications coverage. The measured VSWR result of the primary antenna is presented in Fig. 6, which shows satisfactory VSWR, i.e., less than 2 throughout the UWB spectrum. Fig. 4(a) shows the top view, and Fig. 4(b) shows the bottom view of the primary UWB antenna.

Here three cases are fabricated to verify the simulation results through measurement and presented in Fig. 5.

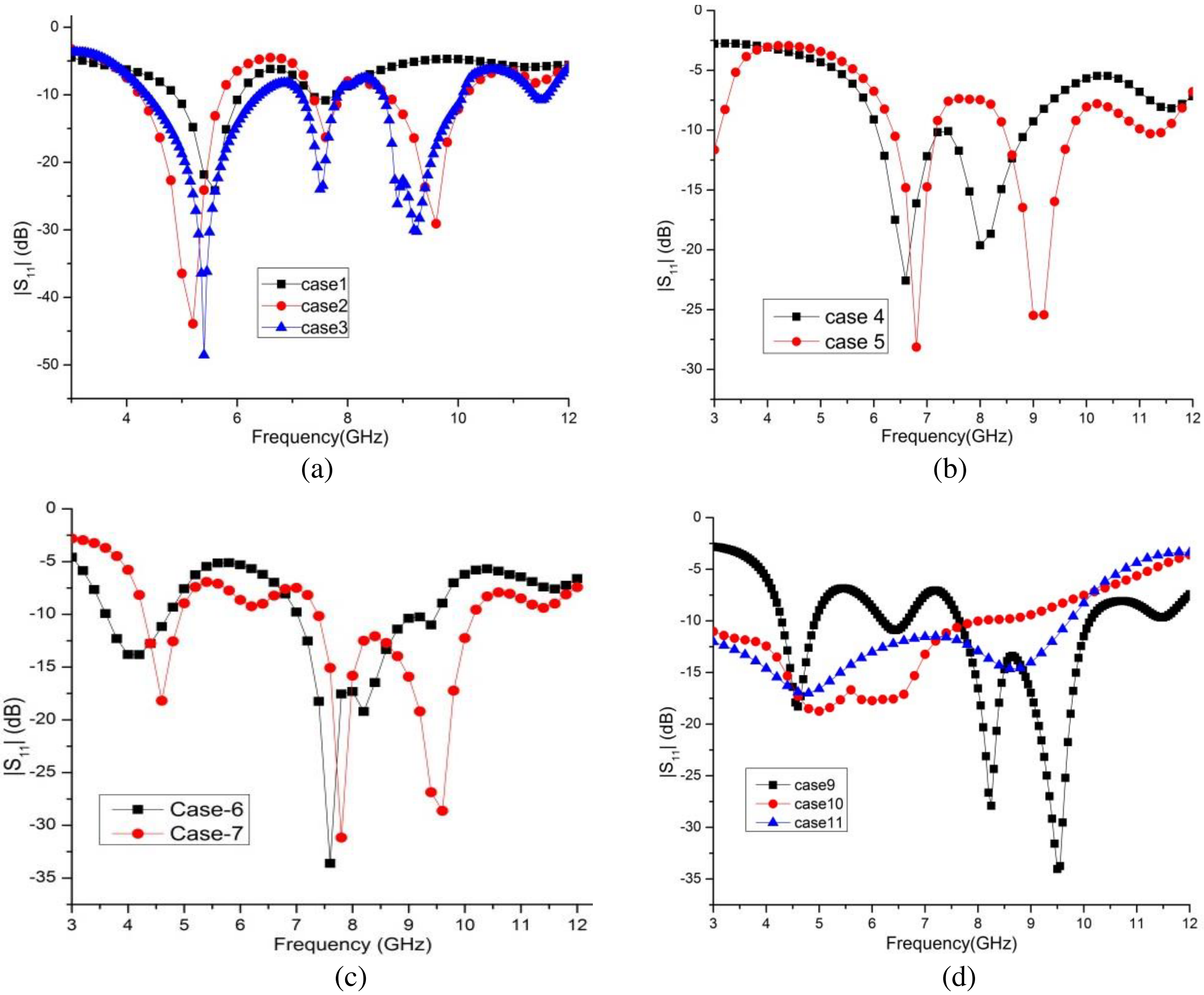

Figure 3. $S_{11}$for Reconfigurable Antennas with distinct diode Configurations. (a) S_{11} for Case-1, Case-2 and Case-3. (b) S_{11} for Case-4 and Case-5. (c) S_{11} for Case-6 and Case-7. (d) S_{11} for Case-9, Case-10 and Case-11.

(a) (b)

Figure 4. Photographs of fabricated prototype of primary UWB antenna. (a) Top view. (b) Bottom view.

4. MEASURED RESULTS OF PROTOTYPE ANTENNAS

Measurements of the primary antenna VSWR and specific cases like Case-1, Case-2 and Case-8 reflection coefficient S_{11} (dB) are performed with Keysight Vector Network Analyzer. The simulated and measured

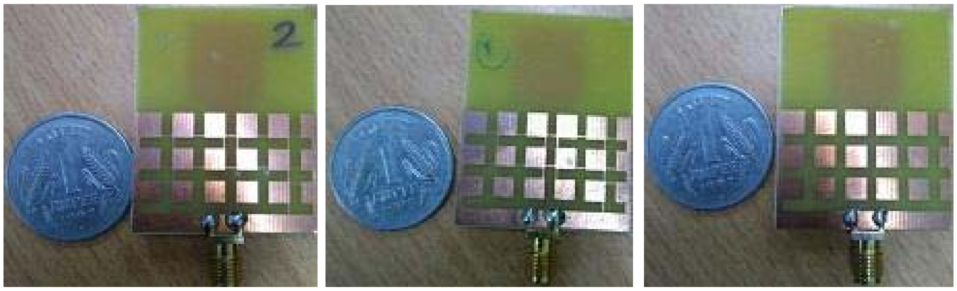

Case-1 Case-2 Case-8

Figure 5. Prototype fabricated examples of Case-1, Case-2 and Case-8. (a) Case-1. (b) Case-2. (c) Case-8.

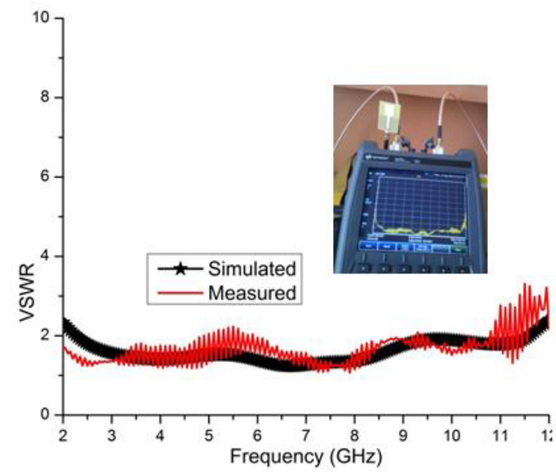

Figure 6. Measured and simulated results of primary antenna. VSWR of primary antenna (UWB antenna).

VSWRs of the primary prototype antenna are presented in Fig. 6 and show excellent agreement with VSWR less 2 throughout the UWB spectrum. In Fig. 7 simulated and measured results of proposed antenna for specific cases like Case-1, Case-2, and Case-8 are presented.

Case-1 simulated and measured S_{11} (dB) results show desired agreement, and the proposed antenna can be applicable to multiband applications like WLAN and X-band satellite communications. Similarly, Case-2 prototype antenna is also applicable to multiband operations.

Case-8 antenna's simulated and measured S_{11} (dB) show desired agreement, and it also verifies that the proposed configuration is a good candidate for the multiband applications in WLAN, X-band satellite communications and ITU systems.

Figure 8 shows the simulated E-field pattern & H-field pattern (co & cross polarization) at 3, 4.6, 5.6, 7, 8 GHz and 9.6 GHz. The proposed antennas show successful multiband creation and broad bandwidth with VSWR < 2. From Figs. 8(a)–(e), it is observed that the antenna displays satisfactory omnidirectional patterns in the H-field similar to dipole like patterns for E-field.

Some useful information of other pixel structured antennas used as reference in this paper is listed in Table 3.

The radiation characteristic of suggested antennas is measured in an anechoic chamber for co & cross polarizations, and results are presented for various frequencies in Fig. 8. There is good agreement between simulated and measured radiation characteristics in both the planes namely XZ (E-Plane) and YZ (H-Plane). The proposed antenna shows identical radiation pattern to the dipole antenna in E-field (XZ plane) and omnidirectional pattern in H-field (YZ plane). Radiation characteristics at

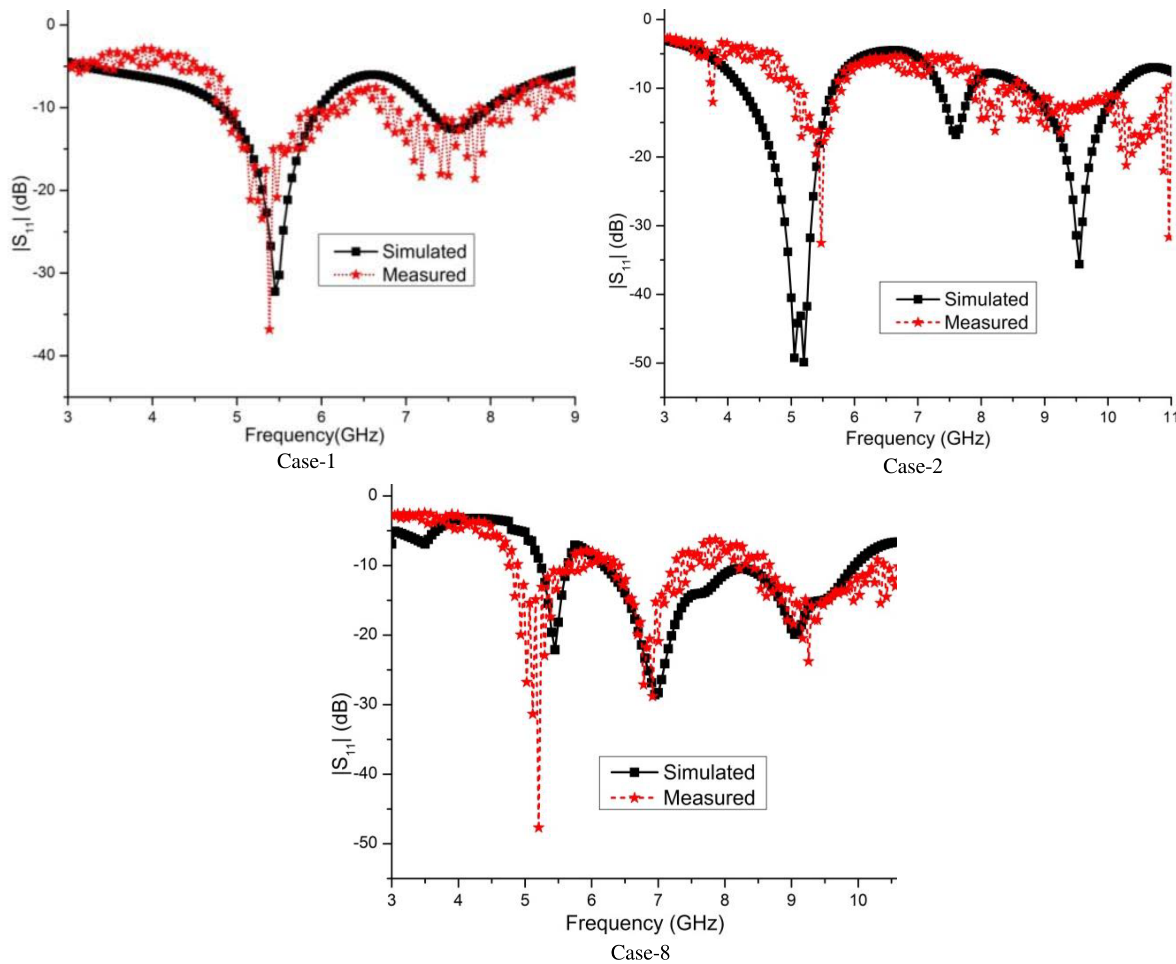

Figure 7. Measured and simulated S_{11} (dB) responses of prototype examples of Case-1, Case-2, and Case-8.

high frequencies deviate from the omnidirectional pattern in E-field due to the appearance of higher order modes.

An external biasing is used to activate PIN diodes for discussed Case-1 antenna configuration. Here we apply 3 volt power supply with $100\,\Omega$ series resistance at the diode input whereas it is grounded through 1.6 pF inductor with power supply negative terminal.

Here we present a prototype of Case-1 (Fig. 9), and its responses are depicted by Fig. 10. Table 4 is used to present various outcomes of simulation and measurement of the antenna with various combinations of diodes.

The antenna configuration in Case-1 is designed using a PIN diode and metal strip to analyze their effects on result. The compared reflection coefficient $|S_{11}|$ results in Fig. 11 show that the antenna with PIN diode configuration has good agreement with simulated result. The antenna configuration with metal strip has significant variation with respect to simulated one. However, the mean percentage error from 3 to 10 GHz is calculated with respect to the simulated result of antenna with a PIN diode and metal strip being 2.5% and 28%, respectively. The discrepancy in results for metal strip method is due to its own radiation and extra resistance values. Moreover, metal strip method is useful for verifying various configurations as it has satisfactory agreement of results with PIN diode integrated antenna.

The measured peak realized gains of three antenna configurations, namely Case-1, Case-2 and Case-8, are presented in Fig. 12. The antenna has low gain due to the pixel ground (primary antenna is a partial ground antenna), and primarily it is a UWB antenna which has limitation of gain.

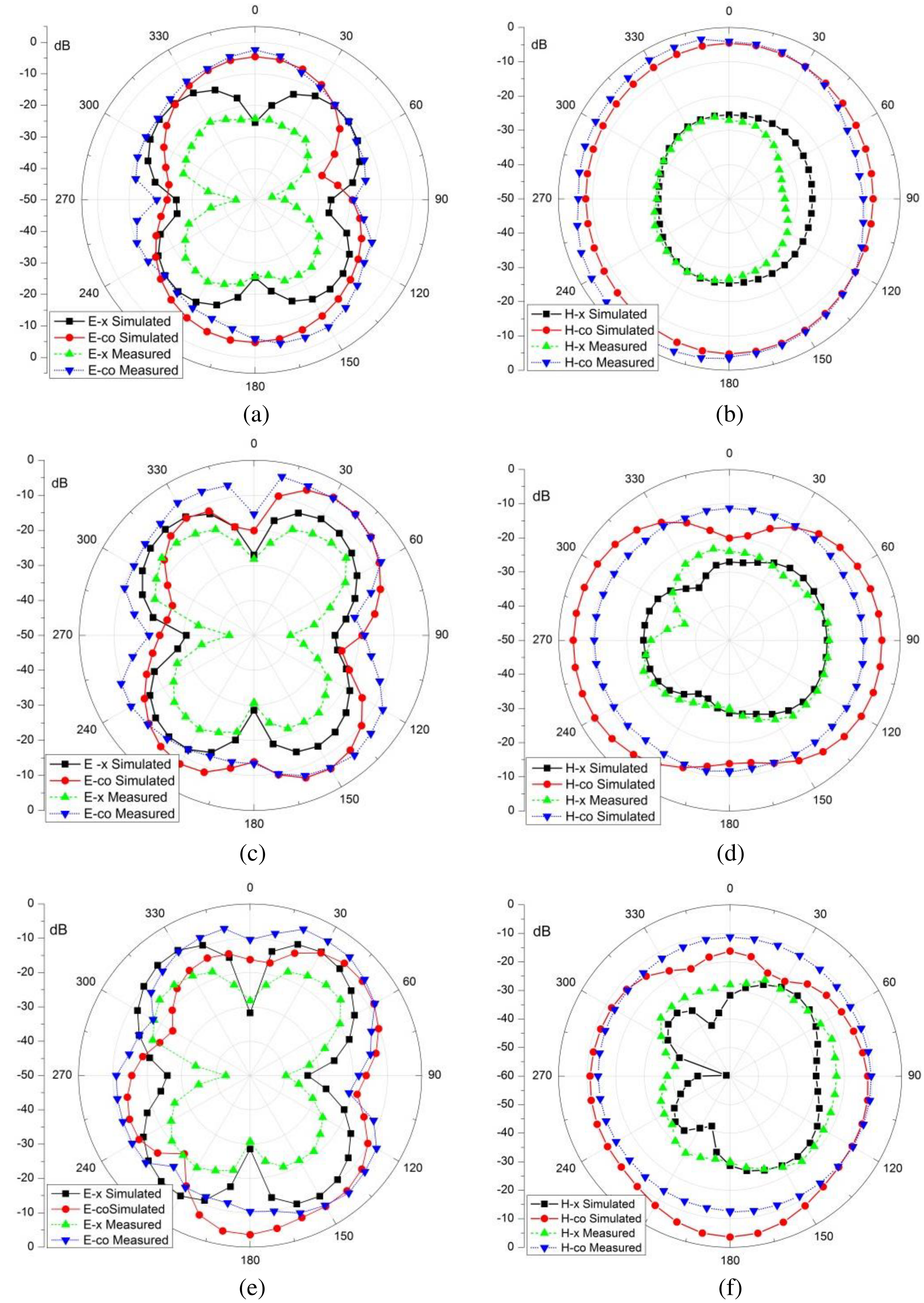

Figure 8. Measured and simulated E-plane pattern and H-plane pattern (co & cross polarization) at various frequencies of proposed antenna. (a) E-plane pattern at 5.6 GHz. (b) H-plane pattern at 5.6 GHz. (c) E-plane pattern at 8 GHz. (d) H-plane pattern at 8 GHz. (e) E-plane pattern at 9 GHz. (f) E-plane pattern at 9 GHz.

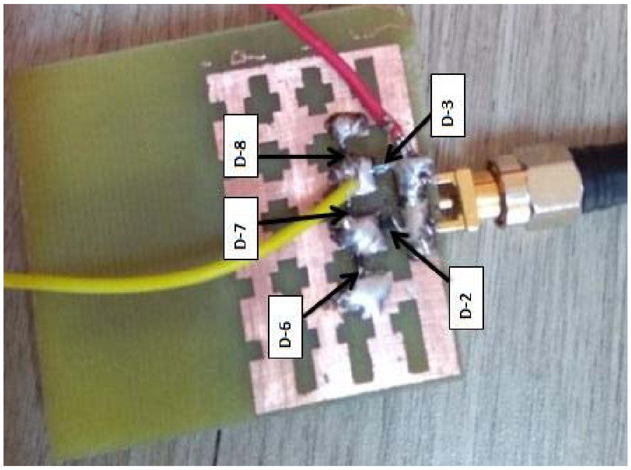

Figure 9. Prototype illustration for Case-1.

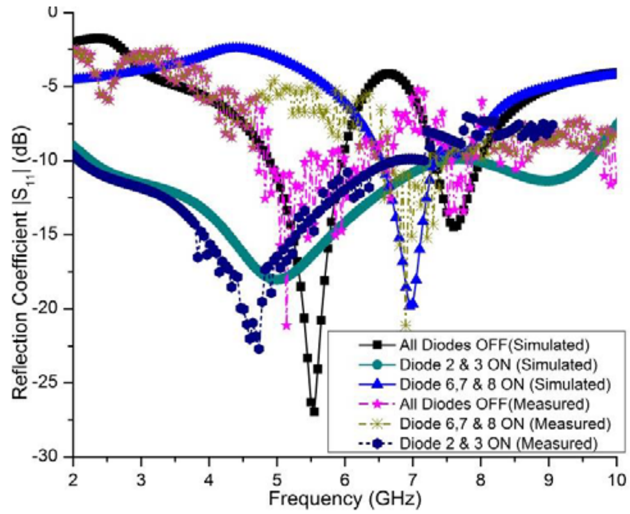

Figure 10. Magnitude of S_{11} (dB) response of prototype example for Case-1.

Table 3. Resonant frequencies for various reconfigurable antennas.

Ref.	Substrate	ε_r	Reconfiguration	Band
1	R03003C	3	Pattern	WLAN
2	Quartz	3.9	Pattern	WLAN
3	RO4003C	3.55	Beam steering and Polarization	WLAN
4	RO4003	3.55	Frequency and Pattern	1–6 GHz
5	RO-TMM3	3.27	Frequency, Pattern and Polarization	4–7 GHz
6	RT/Duroid 5880	3.9	Frequency and Pattern	10 GHz
7	RO4003	3.55	Frequency	1–2 GHz
8	Glossy Paper	3.2	Frequency	9.50 MHZ, 2.45 and 5.2 GHz
9	FR-4	4.4	Frequency	820–2300 MHz
10	RO4003	3.55	Frequency	4–7 GHz
11	NA	NA	Frequency and Pattern	2 to 4 GHz
12	Microwave Laminator	3.35	Pattern	4.8–5.2 GHz
13	RO4003	3.55	Pattern	2.5 GHz
14	NA	NA	Frequency	1.3 GHz
15	RO4003	3.55	Frequency	S-band
*	FR-4	4.4	Frequency	Single and Multiband

* Present Work
NA Not Available

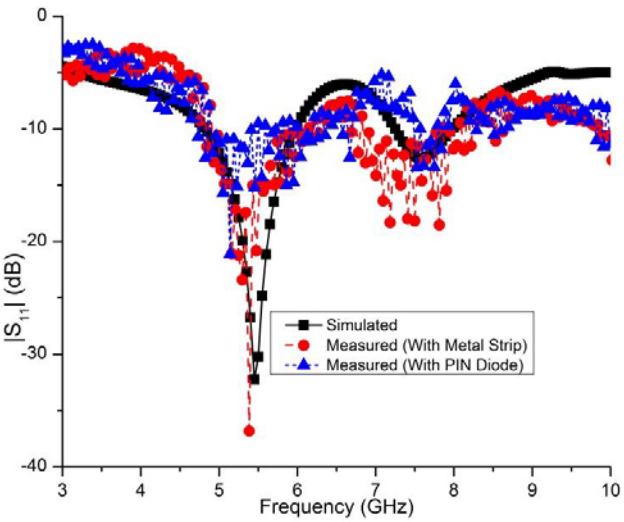

Figure 11. $|S_{11}|$ performance of antenna configuration in Case-1 using metal strip and PIN diode.

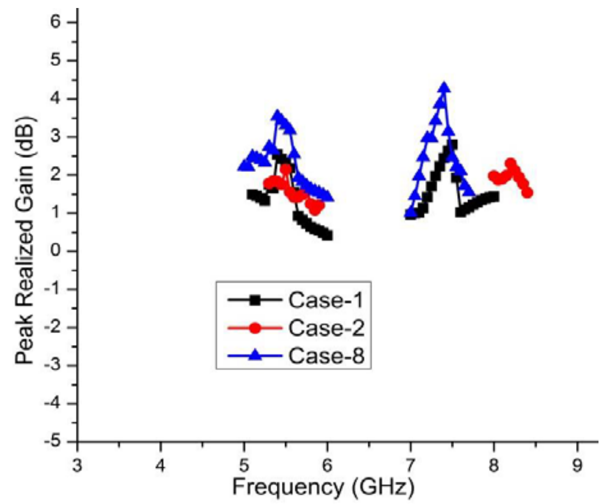

Figure 12. Measured peak realized gains for prototype antenna for Case-1, 2 and 8.

Table 4. Case-1 diode position study and responses.

Diodes	Simulated Band (GHz)	Measured Band (GHz)
All diodes (OFF)	5–6 GHz, 7.3–8.3 GHz	5–5.8 GHz, 7.2–8.2 GHz
Diode 6, 7 & 8 (ON)	6.5–7.5 GHz	6.5–7.8 GHz
Diode 2 & 3 (ON)	2–8 GHz	2–8 GHz

5. CONCLUSION

Initially the primary antenna with partial ground is simulated, fabricated and measured, which operates over UWB (3.1 to 10.6 GHz) spectrum and it reflects a respectable agreement between simulation and measurement VSWR $<$ 2 throughout UWB spectrum. The pixel ground concept has been well verified through three specific cases which successfully are operated over multiband, single band and UWB spectrum. The measured prototype cases have desired agreement with simulated results, and it also verifies that pixel ground structure plays a great role to produce reconfigurable antennas for multiband functioning antennas. Results & analysis of this antenna indicate that implementation of pixel ground approach to achieve frequency reconfiguration is useful where biasing of switches is not favorable. However, pixel ground reconfigurable antennas have disadvantages of huge number of RF switches which increases the cost of complete systems. The analysis of proposed antenna configuration successfully demonstrates the multiband and wide-band functionality.

ACKNOWLEDGMENT

We are thankful to Prof. Kumar Vaibhav Srivastava of Indian Institute of Technology, Kanpur, India for providing the measuring facility for radiation pattern measurement in RF microwave lab and anechoic chamber. Authors are also thankful to Global Institute of Technology, Jaipur, Rajasthan (INDIA) for providing measuring facilities like VNA (up to 14 GHz).

REFERENCES

1. Lotfi, P., S. Soltani, and R. D. Murch, "Broadside beam-steerable planar parasitic pixel patch antenna," *IEEE Trans. Antennas Propag.*, Vol. 64, No. 10, 4519–4524, Oct. 2016.
2. Yuan, X., et al., "A parasitic layer-based reconfigurable antenna design by multi-objective optimization," *IEEE Trans. Antennas Propag.*, Vol. 60, No. 6, 2690–2701, Jun. 2012.
3. Li, Z., D. Rodrigo, L. Jofre, and B. A. Cetiner, "A new class of antenna array with a reconfigurable element factor," *IEEE Trans. Antennas Propag.*, Vol. 61, No. 4, 1947–1955, Apr. 2013.
4. Rodrigo, D. and L. Jofre, "Frequency and radiation pattern reconfigurability of a multi-size pixel antenna," *IEEE Trans. Antennas Propag.*, Vol. 60, No. 5, 2219–2225, May 2012.
5. Besoli, A. G. and F. D. Flaviis, "A multifunctional reconfigurable pixeled antenna using MEMS technology on printed circuit board," *IEEE Trans. Antennas Propag.*, Vol. 59, No. 12, 4413–4424, Dec. 2011.
6. Rodrigo, D., Y. Damgaci, M. Unlu, B. A. Cetiner, J. Romeu, and L. Jofre, "Antenna reconfigurability based on a novel parasitic pixel layer," *Proceedings of the 5th European Conference on Antennas and Propagation (EUCAP)*, 3497–3500, 2011,
7. Bishop, N., M. Ali, W. Baron, J. Miller, J. Tuss, and D. Zeppettella, "Aperture coupled MEMS reconfigurable pixel patch antenna for conformal load bearing antenna structures (CLAS)," *2014 IEEE Antennas and Propagation Society International Symposium (APSURSI)*, 1091–1092, 2014.
8. Mansour, A. M., et al., "Compact reconfigurable multi-size pixel antenna for cognitive radio networks and IoT environments," *2016 Loughborough Antennas Propagation Conference (LAPC)*, 1–5, 2016.
9. Song, S. and R. D. Murch, "An efficient approach for optimizing frequency reconfigurable pixel antennas using genetic algorithms," *IEEE Trans. Antennas Propag.*, Vol. 62, No. 2, 609–620, Feb. 2014.
10. Ali, M., N. Bishop, W. Baron, B. Smyers, J. Tuss, and D. Zeppettella, "A MEMS reconfigurable pixel microstrip patch antenna for conformal load bearing antenna structures (CLAS) concept," *2014 IEEE Antennas and Propagation Society International Symposium (APSURSI)*, 1093–1094, 2014.
11. Muscat, A. and J. A. Zammit, "An efficient algorithm for the control of reconfigurable pixel microstrip antennas," *2009 Second International Conference on Advances in Circuits, Electronics and Micro-electronics*, 44–47, 2009.
12. Rodrigo, D., J. Romeu, and L. Jofre, "Interference rejection using frequency and pattern reconfigurable antennas," *Proceedings of the 2012 IEEE International Symposium on Antennas and Propagation*, 1–2, 2012.
13. Hossain, M. A., I. Bahceci, and B. A. Cetiner, "Parasitic layer-based radiation pattern reconfigurable antenna for 5G communications," *IEEE Trans. Antennas Propag.*, Vol. 65, No. 12, 6444–6452, Dec. 2017.
14. Lotfi, P., S. Soltani, and R. D. Murch, "Printed endfire beam-steerable pixel antenna," *IEEE Trans. Antennas Propag.*, Vol. 65, No. 8, 3913–3923, Aug. 2017.
15. Rodrigo, D., E. Diaz, and L. Jofre, "Reconfigurable pixel-layer isolator for frequency-tunable on-frequency repeaters," *IEEE Antennas Wirel. Propag. Lett.*, Vol. 13, 475–478, 2014.
16. Tewari, M., A. Yadav, and R. P. Yadav, "Frequency reconfigurable antenna: Using pixel ground," *2016 International Conference on Recent Advances and Innovations in Engineering (ICRAIE)*, 1–6, 2016.
17. Trinh-Van, S. and C. Dao-Ngoc, "Dual band-notched UWB antenna based on electromagnetic band gap structures," *REV J. Electron. Commun.*, Vol. 1, Sep. 2011.
18. Kishore, N., A. Prakash, and V. S. Tripathi, "A reconfigurable ultra wide band antenna with defected ground structure for ITS application," *AEU — Int. J. Electron. Commun.*, Vol. 72, 210–215, Feb. 2017.